

Contents lists available at ScienceDirect

Petroleum Science

journal homepage: www.keaipublishing.com/en/journals/petroleum-science



Original Paper

Fracture geometry and breakdown pressure of radial borehole fracturing in multiple layers



Yu-Ning Yong ^a, Zhao-Quan Guo ^b, Shou-Ceng Tian ^{a, *}, Lu-Yao Ma ^c, Tian-Yu Wang ^a, Mao Sheng ^a

- ^a National Key Laboratory of Petroleum Resources and Engineering, China University of Petroleum (Beijing), Beijing, 102249, China
- ^b Beijing Petroleum Machinery Company Limited, CNPC Engineering Technology R&D Company Limited, Beijing, 102206, China
- ^c Smart Energy Co., Ltd, China Xiongan Group, Xiong'an New Area, 071000, Hebei, China

ARTICLE INFO

Article history: Received 2 March 2023 Received in revised form 11 September 2023 Accepted 13 September 2023 Available online 18 September 2023

Edited by Yan-Hua Sun

Keywords: Multi-layer radial boreholes Hydraulic fracturing Fracture propagation Pressure characteristic

ABSTRACT

Radial borehole fracturing that combines radial boreholes with hydraulic fracturing is anticipated to improve the output of tight oil and gas reservoirs. This paper aims to investigate fracture propagation and pressure characteristics of radial borehole fracturing in multiple layers. A series of laboratory experiments with artificial rock samples (395 mm × 395 mm × 395 mm) was conducted using a true triaxial fracturing device. Three crucial factors corresponding to the vertical distance of adjacent radial borehole layers (vertical distance), the azimuth and diameter of the radial borehole are examined. Experimental results show that radial borehole fracturing in multiple layers generates diverse fracture geometries. Four types of fractures are identified based on the connectivity between hydraulic fractures and radial boreholes. The vertical distance significantly influences fracture propagation perpendicular to the radial borehole axis. An increase in the vertical distance impedes fracture connection across multiple radial borehole layers and reduces the fracture propagation distance along the radial borehole axis. The azimuth also influences fracture propagation along the radial borehole axis. Increasing the azimuth reduces the guiding ability of radial boreholes, which makes the fracture quickly curve to the maximum horizontal stress direction. The breakdown pressure correlates with diverse fracture geometries observed. When the fractures connect multi-layer radial boreholes, increasing the vertical distance decreases the breakdown pressure. Decreasing the azimuth and increasing the diameter also decrease the breakdown pressure. The extrusion force exists between the adjacent fractures generated in radial boreholes in multiple rows, which plays a crucial role in enhancing the guiding ability of radial boreholes and results in higher breakdown pressure. The research provides valuable theoretical insights for the field application of radial borehole fracturing technology in tight oil and gas reservoirs.

© 2023 The Authors. Publishing services by Elsevier B.V. on behalf of KeAi Communications Co. Ltd. This is an open access article under the CC BY-NC-ND license (http://creativecommons.org/licenses/by-nc-nd/

4.0/).

1. Introduction

Tight oil and gas are essential unconventional resources globally, and hydraulic fracturing has been the main technology for their extraction in the last decades (Sun et al., 2010; Zou et al., 2018). However, certain reservoirs might not achieve sufficient stimulation through hydraulic fracturing, resulting in a production that falls short of expectations (Liu and Ehlig-Economides, 2016; Guo et al., 2019; Sun et al., 2019). Ultrashort-radius radial borehole

* Corresponding author.

E-mail address: tscsydx@163.com (S.-C. Tian).

(briefly radial borehole) drilling is a new technology formed in recent decades (Landers, 1998; Kamel, 2016; Huang et al., 2020a, 2020b). This technology drills one or more lateral boreholes radially along the vertical wellbore. The diameters of radial boreholes range from 20 to 50 mm and their lengths are about 10–100 mm. Radial borehole drilling was initially applied to low coal rank reservoirs, resulting in a significant increase in single-well coalbed methane production by 5–6 times. However, relying on this technology for achieving economic commercial exploitation of reservoirs still presents challenges (Xian et al., 2010). Therefore, scholars proposed radial borehole fracturing, a combination of radial borehole drilling and hydraulic fracturing, to improve the conductivity between radial boreholes and reservoirs (Wu, 2012). The process of radial

borehole fracturing is as follows: firstly, radial boreholes in multiple layers are drilled along the vertical main wellbore; then the radial boreholes are hydraulically fractured; and finally, a complex fracture network is generated in the reservoir, as shown in Fig. 1. Radial borehole fracturing technology has been successfully applied in several countries with a good effect (Li et al., 2000; Bruni et al., 2007; Cirigliano and Talavera Blacutt, 2007; Cinelli and Kamel, 2013; Ragab and Kamel, 2013; Maut et al., 2017). Therefore, radial borehole fracturing is anticipated to enhance the productivity of tight oil and gas reservoirs compared to conventional hydraulic fracturing.

Several studies were carried out to investigate initiation and propagation of fractures in radial borehole fracturing. Regarding the research on fracture initiation in radial borehole fracturing, Gong et al. (2016) analyzed the influence of several factors on the fracture initiation pressure and position of radial borehole fracturing using ABAQUS. Wang et al. (2020) also investigated the effects of azimuth, radial borehole branch, and in-situ stress on fracture initiation pressure and position, emphasizing that azimuth is critical for multi-fracture propagation. Besides, Liu and Tian (2020) analyzed the effects of various factors on fracture initiation in two layouts where a radial borehole was drilled from either a vertical or horizontal main wellbore. Bai et al. (2021) developed an analytical model to predict stress distribution around a vertical wellbore that contains multiple radial boreholes of arbitrary dip angles and azimuths. They investigated the influences of a series of parameters on fracture initiation pressure, fracture initiation position, and stress distribution. Regarding the research on fracture propagation in radial borehole fracturing, Guo et al. (2016, 2017b) established a numerical model for hydraulically fracturing a single radial borehole and radial boreholes in a row (the axes of radial boreholes distributed in a vertical plane). The results indicated that a single radial borehole, particularly when arranged in a row with several others, can affect the in-situ stress around the boreholes and promote hydraulic fractures to propagate preferentially along their axes, which is called the "guiding ability" of radial boreholes. Besides, the effects of ten factors (the azimuth, diameter, and length of radial borehole, the viscosity of the fracturing fluid, the horizontal stress difference, and so on) on fracture propagation were investigated. Tian et al. (2017) derived a criterion for the propagation of fractures in a row of radial boreholes under in-situ stress and suggested optimizing the borehole spacing to improve efficiency and economy. Based on the extended finite element method, Guo et al. (2019) investigate fracture propagation in two branches of radial boreholes in the same layer. The results showed that increasing the

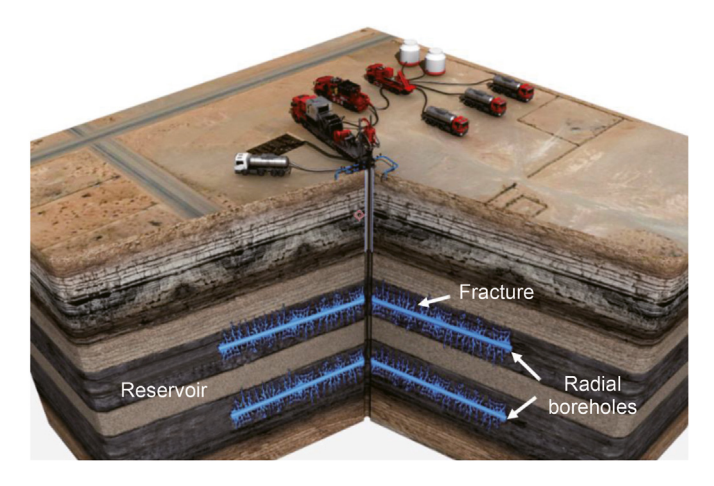


Fig. 1. Schematic of radial borehole fracturing in multiple layers.

azimuth and the horizontal stress difference can sharply reduce the guiding ability of radial boreholes. Using the same method, Liu et al. (2019) conducted a more detailed investigation on the influence of seven factors on the directional propagation of fractures in radial borehole fracturing, subsequently ranking these factors in order of their relative impact.

Laboratory experiments have also been conducted to study radial borehole fracturing. Fu et al. (2015) performed experiments on coal and observed that increases in both the length and the number of branches of radial boreholes decrease the breakdown pressure. This finding was also confirmed by a numerical simulation conducted by Liu et al. (2018a). Yan et al. (2017) carried out triaxial hydraulic fracturing experiments on artificial samples with a single radial borehole and discovered that increasing the azimuth results in higher breakdown pressure and fracture extension pressure, and creates more complex fractures. Guo et al. (2017a) first implemented the fracturing experiment of radial boreholes in a row, confirming the possibility of directional propagation of fractures guided by multiple radial boreholes. Furthermore, Guo et al. (2019) employed a comprehensive approach combining theoretical analysis, numerical simulation, and experimental investigation to demonstrate that rationally arranging the layout of radial boreholes can create multiple fractures. Guo et al. (2022) conducted experiments to investigate the influence of the radial borehole parameters on fracture geometries in multi-branch radial borehole fracturing. They found that the horizontal zones between adjacent radial boreholes exhibit extrusion forces, which affects fracture propagation and breakdown pressure.

The radial borehole fracturing technology typically entails fracturing multi-layer and multi-branch radial boreholes in the reservoir. However, current research on radial borehole fracturing has mainly concentrated on the layout of a single radial borehole or several radial boreholes within a single layer or row. As a result, there is a limitation in investigating fracture propagation in radial boreholes with multiple branches and layers. Additionally, the analysis of results has primarily focused on fracture propagation parallel to the radial borehole axes, while further research is necessary to investigate fracture propagation perpendicular to the radial borehole axes. This work aims to analyze the fracture geometry and pressure characteristics of radial borehole fracturing in multiple layers through laboratory experiments, with a specific focus on fracture propagation perpendicular to the radial borehole axes. Three crucial factors corresponding to the vertical distance of adjacent radial borehole layers (vertical distance), the radial borehole azimuth and diameter are examined. In the following sections, we will introduce the experiment, present and discuss the results, and draw some conclusions.

2. Experimental

2.1. Preparation of samples

The experimental samples with the dimensions of $395 \text{ mm} \times 395 \text{ mm} \times 395 \text{ mm}$ are artificial rocks comprised of the matrix and wellbores. The matrix is a uniformly mixed cement mortar, which consists of Ordinary 42.5R Portland cement, sand (40–80 mesh), and water, with a mass ratio of 100: 90: 31. The preparation method of samples is as follows: initially, the wellbore is secured at the center of a steel mold. Subsequently, the matrix is poured into the mold, and finally, the upper surface of the matrix is smoothed using a cement scraper, as illustrated in Fig. 2. After standing still for 24 h, the solidified sample can be taken out after disassembling the mold. The artificial rock sample used in the experiment is shown in Fig. 3(a) and (b). To maintain the consistent strength and properties of samples and to prevent the development

Y.-N. Yong, Z.-Q. Guo, S.-C. Tian et al. Petroleum Science 21 (2024) 430–444



Fig. 2. The process of casting rock samples.

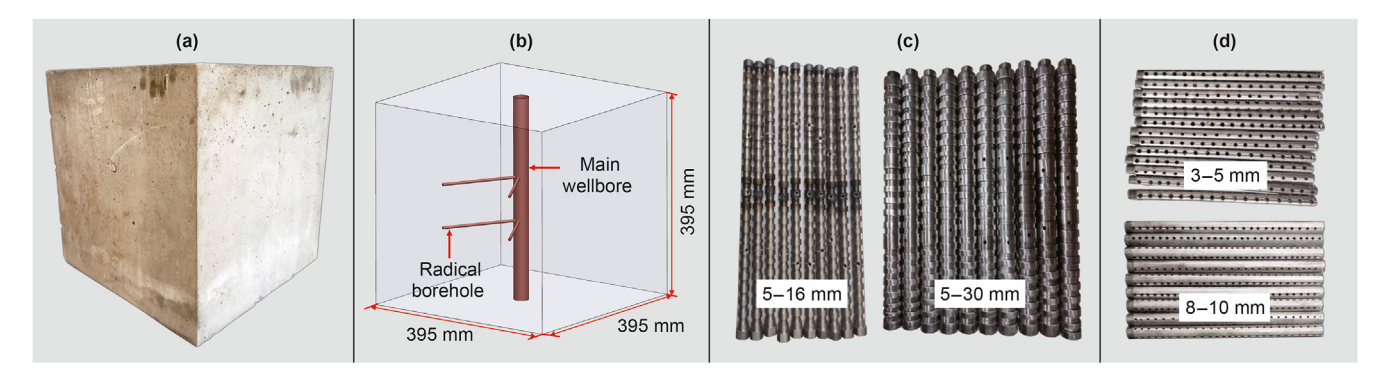


Fig. 3. The rock samples and wellbores.

of cracks caused by dehydration during cement hydration, all samples were stored at room temperature for 28 days and watered every two days (Raheem et al., 2013). To evaluate the mechanical properties of the samples, small concrete blocks were also prepared and tested, with detailed results shown in Guo et al. (2022).

The wellbores comprise the main wellbore and radial boreholes. The main wellbore has a length of 412 mm and two sets of innerouter diameter (I-OD) of 5-30 mm and 5-16 mm, respectively (Fig. 3(c)). Previous research has proved that the stress zone caused by the wellbore vanishes within four times their diameters (Abass et al., 2009). Hence, the length of radial boreholes should exceed four times the diameter of the main wellbore, while also ensuring a sufficient distance between the radial borehole ends and the boundaries of the samples. The dimensions of three sets of radial boreholes are as follows: 150 mm long with I-OD of 3-5 mm, 150 mm long with I-OD of 8-10 mm, and 130 mm long with I-OD of 3-5 mm (Fig. 3(d)). The radial boreholes with a length of 150 mm are linked to the main wellbore with I-OD of 5-30 mm, while those with a length of 130 mm are connected to the main wellbore with I-OD of 5-16 mm. To simulate an open radial borehole. several small holes were drilled into the radial boreholes and thin membranes were coated on their surface to avoid mortar entering the radial boreholes during casting (Liu et al., 2018b). The main wellbore and the radial wellbores are linked using threads. Specifically, an internal thread is cut at a specific position of the main wellbore, and an external thread is processed at one end of the radial wellbores.

The fracturing fluid used is a mixture of glycerin and water with a mass ratio of 1:4. To enhance the identification of the fracture surface, a little red ink is added to the fracturing fluid. The viscosity of the fracturing fluid is measured to be 40 mPa s (Guo et al., 2022).

2.2. Experimental device and procedures

Fig. 4 presents the schematic of the experimental device, a true triaxial fracturing apparatus. The duplex syringe pump can inject fluids at a maximum speed of 100 mL/min. The fracturing chamber that contains six plates is used to fix the samples. The confining pressure is applied to the samples by the confining pressure loading unit, which can provide an oil pressure of up to 60 MPa. It is noted that the confining pressure needs to be converted from the oil pressure according to the plate size. The automatic control and data collection system controls the pump and confining pressure loading unit and collect the experimental data at a sampling rate of 1000 Hz and an accuracy of 0.1.

All the samples are fractured by the same experimental procedures. Before fracturing, the sample is fixed in the fracture chamber with six plates. To simulate realistic subsurface pressure conditions, a tri-axial confining pressure is imposed on the sample using the confining pressure loading unit. Fracturing fluid is then injected into the main wellbore by duplex syringe pumps. The injection process will stop when the fracturing fluid leakage is observed from the sample surface. After fracturing, the sample is taken out and carefully opened with a sharp iron chisel along the fracture contours. The hydraulic fracture is observed and measured.

2.3. Experimental scheme

The vertical distance between adjacent radial borehole layers (vertical distance), the azimuth and diameter of the radial borehole are considered to investigate fracture propagation and pressure characteristics of radial borehole fracturing in multiple layers. Some factors are defined and illustrated in Fig. 5. The experiments

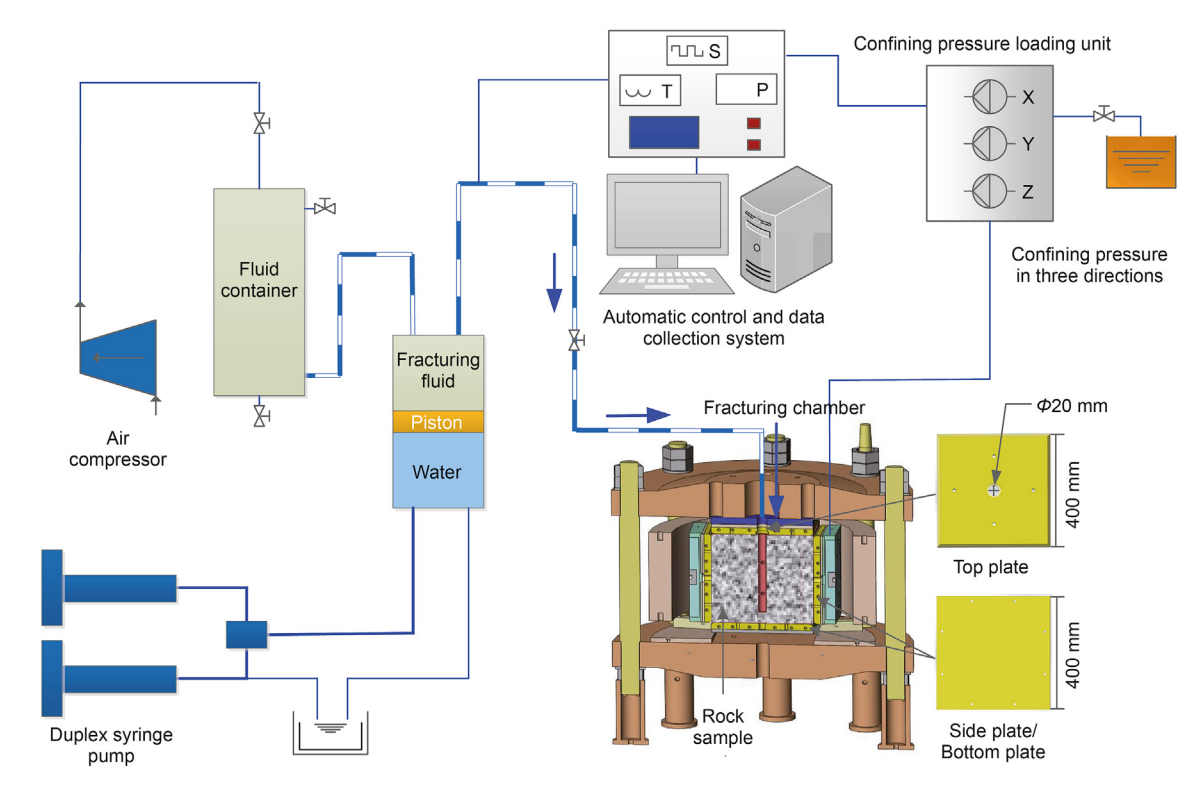


Fig. 4. Schematic of the true triaxial fracturing apparatus.

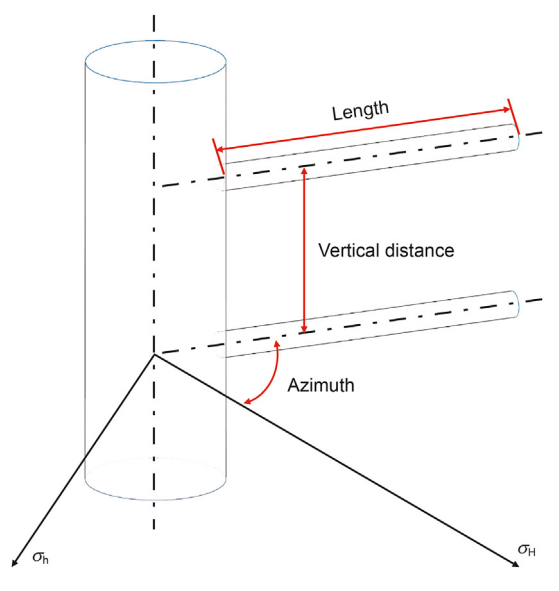


Fig. 5. Schematic of the radial borehole parameters.

are classified into two main groups based on the radial borehole layout (two and three layers). Each group consists of several sets with varying vertical distances. The experimental scheme for the two layouts considers the potential influence of rock boundaries on the radial boreholes. Specifically, for the two radial borehole layers, both are always positioned adjacent to rock boundaries, while for the three radial borehole layers, the middle radial borehole layer is situated next to other radial borehole layers. Additionally, increasing the vertical distance weakens the stress superposition between vertical radial boreholes, reducing the effect of radial boreholes on fractures (Tian et al., 2017). The experimental results

are more susceptible to interference from rock boundaries. To address these factors and ensure the reliability and accuracy of the obtained results, repeated experiments were conducted specifically when the vertical distance reached its maximum value in each experimental set. The normal fault stress state is set at 25/17/12 MPa (Liu et al., 2018b), and the pump rate is set at 30 mL/min for all experiments. Other experimental parameters are listed in Table 1.

3. Result and analysis

This section presents and analyzes the results concerning fracture geometries and breakdown pressures of samples that were fractured with two and three radial borehole layers, respectively. The characterization of fracture geometries is analyzed both qualitatively and quantitatively in this study. The qualitative analysis of the fracture depends on the fracture reconstructed by SOLID-WORKS. After the samples are opened along the fracture contours on the sample surface, fractures can be identified through observation of their surface color and roughness, which appear light red due to the addition of red ink to the fracturing fluid and are smoother than fractures produced by manual gouging, as shown in Fig. 6. When the fracture is judged, a 3D image can be drawn in SOLIDWORKS through the spatial shape of the fractures in the sample. To quantify fracture geometries, the deviation distance is quoted, which was introduced by Guo et al. (2022). The deviation distance refers to the distance between the point where the hydraulic fracture deviates from the radial borehole and the point where the radial borehole axis intersects with the outer wall of the main wellbore, as shown in Fig. 7. The breakdown pressure is defined as the maximum value of the fracturing curve. Fig. 8 shows the typical fracturing curve for radial borehole fracturing, where the breakdown pressure is measured at 23.2 MPa.

Y.-N. Yong, Z.-Q. Guo, S.-C. Tian et al. Petroleum Science 21 (2024) 430—444

 Table 1

 Experimental parameters of radial borehole fracturing in multiple layers.

| Test number | Azimuth of radial boreholes, degree | Vertical distance of radial borehole layers, mm | Diameter of radial boreholes, mm | Length of radial boreholes, mm | Number of radial borehole layers | Number of radial boreholes |
|----------------|-------------------------------------|---|----------------------------------|--------------------------------|----------------------------------|----------------------------|
| 1-1 | 30 | 60 | 5 | 150 | 2 | 4 |
| 1-2 | | 80 | | | | |
| 1-3 | | 100 | | | | |
| 1-4 | | 120 | | | | |
| 1-5 | | 120 | | | | |
| 1-6 | 60 | 60 | 5 | 150 | 2 | 4 |
| 1-7 | | 80 | | | | |
| 1-8 | | 100 | | | | |
| 1-9 | | 120 | | | | |
| 1-10 | | 120 | | | | |
| 1-11 | 30 | 80 | 10 | 150 | 2 | 4 |
| 1-12 | | 100 | | | | |
| 1-13 | | 120 | | | | |
| 1-14 | | 120 | | | | |
| 1-15 | 60 | 80 | 10 | 150 | 2 | 4 |
| 1-16 | | 100 | | | | |
| 1-17 | | 120 | | | | |
| 1-18 | | 120 | | | | |
| 2-1 | 30 | 60 | 5 | 130 | 3 | 6 |
| 2-2 | | 80 | | | | |
| 2-3 | | 100 | | | | |
| 2-4 | | 100 | | | | |
| 2-5 | 60 | 60 | 5 | 130 | 3 | 6 |
| 2-6 | | 80 | | | | |
| 2-7 | | 100 | | | | |
| 2-8 | | 100 | | | | |

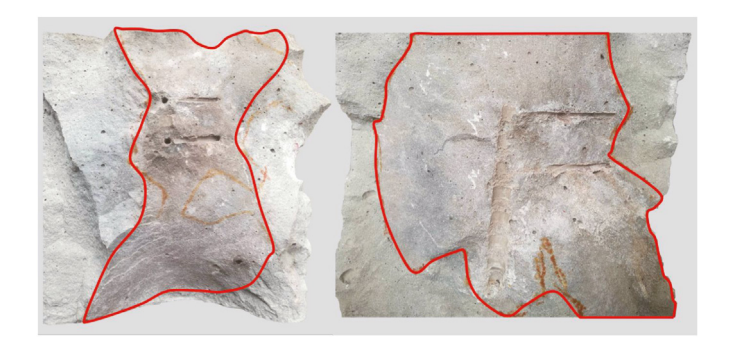


Fig. 6. The results of fracture recognition (the red curves represent fracture contours).

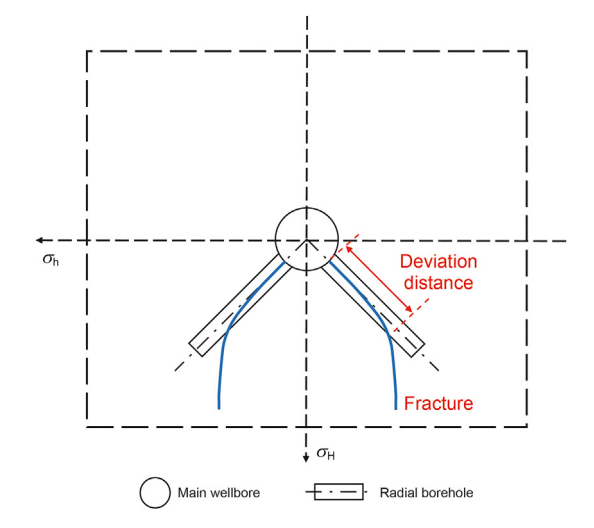


Fig. 7. The definition of deviation distance.

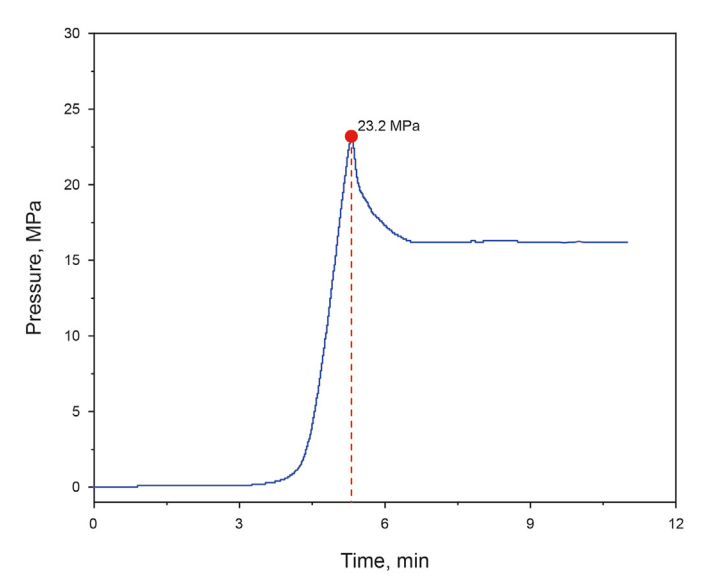


Fig. 8. Typical fracturing curve for radial borehole fracturing.

3.1. Radial borehole fracturing in two layers

3.1.1. Effect of the vertical distance and the azimuth

Previous research has shown that vertical distance has a significant effect on fracture geometries and breakdown pressures (Tian et al., 2017; Guo et al., 2022). In this set of experiments, we investigate the effects of four different vertical distances (60, 80, 100, and 120 mm) with two different azimuths (30° and 60°), while keeping all other parameters constant. The analysis presented in this section includes the characterization of fracture geometries, deviation distances, and breakdown pressures.

Fracture geometries. When the azimuth is 30°, similar fractures are formed with different vertical distances. On the side of the

samples with radial boreholes, fractures that connect two layers of radial boreholes in one row are developed (Fig. 9(a)-(d)). On the side of the samples without radial boreholes, flat fractures initiate from the main wellbore and propagate toward the maximum horizontal stress direction. Since this paper aims to investigate the influence of radial boreholes on fracture propagation, the following description will only focus on the fractures that occur on the side of the samples with radial boreholes. As the vertical distance is 60 mm, the fracture that passes through two radial borehole layers extends straight to the upper and lower boundaries of the sample. When the vertical distances are 80 and 100 mm, the fractures only pass through the heel of the single radial borehole in the bottom layer. As the vertical distance rises to 120 mm, the crooked fracture becomes the largest in this set of experiments. The fracture possibly only passes through the single radial borehole in the bottom layer (Fig. 9(e)). Additionally, to facilitate the connection between the wellbore and the fracturing fluid injection pipeline, a free surface with a diameter of 20 mm is positioned in the middle of the top plate of the triaxial fracturing apparatus (Fig. 4). The presence of the free surface influences the fracture geometries. Consequently, crooked fractures are generated at the top of samples, and their magnitude increases with increasing the vertical distance.

When the azimuth is 60°, fracture geometries are mainly affected by the vertical distance. When the vertical distance is 60 mm, the fractures connect two layers of radial boreholes in two rows and curve to the minimum horizontal stress direction (Fig. 10(a)). When the vertical distance is 80 mm, the fracture passes through two layers of radial boreholes in one row (Fig. 10(b)). As the vertical distance increases to 100 mm, the fracture only passes through a single radial borehole in the top layer (Fig. 10(c)). When the vertical distance rises to 120 mm, the fractures cut through two radial boreholes layers and rapidly curve to the maximum horizontal stress direction (Fig. 10(d) and (e)).

Besides, for sample 1-9# a short fracture propagating a short distance along the axis of the bottom radial borehole is formed, and for sample 1-10# a short fracture is generated in the middle of two radial boreholes, which also extends a short distance along the direction of the radial borehole axis.

Deviation distances. The deviation distances of samples 1-1# to 1-10# are shown in Fig. 11. Increasing the vertical distance reduces the deviation distances. For azimuths of 30° and 60°, as the vertical distance rises from 60 to 120 mm, the deviation distances decrease from 164.2 to 142.9 mm and from 150 to 42.5 mm, respectively. The deviation distances of fractures that extend along a single radial borehole are larger than those of fractures passing through two radial borehole layers (146.8 mm of sample 1-5#, 142.9 mm of sample 1-4#). In sample 1-8#, the fracture only propagates along the top radial borehole and does not reach the bottom boundary of the rock, so the deviation distance is distinctly large. Furthermore, the deviation distances are generally higher when fracturing radial boreholes with the azimuth of 30° compared to 60°.

Breakdown pressures. The fracturing curves and breakdown pressures of samples 1-1# to 1-10# are presented in Figs. 12 and 13. The fracturing curve of sample 1-2# differs significantly from the others due to a pump rate error. Specifically, the pump rate was mistakenly set at 100 mL/min at the start of the experiment. At the second minute, the pump rate was adjusted to 30 mL/min, as shown in the point where the abrupt curvature changed in Fig. 12. The fracturing curve of sample 1-9# is constructed because the fracturing fluid was exhausted in the process of fracturing. The experiment was suspended to add the fracturing fluid.

Owing to an inadvertent error during the experiment, the breakdown pressure of sample 1-2# is deemed invalid, so the following discussion of the breakdown pressure will exclude sample 1-2#. For samples with the azimuth of 30°, the maximum and minimum breakdown pressures are 24.3 and 21.5 MPa,

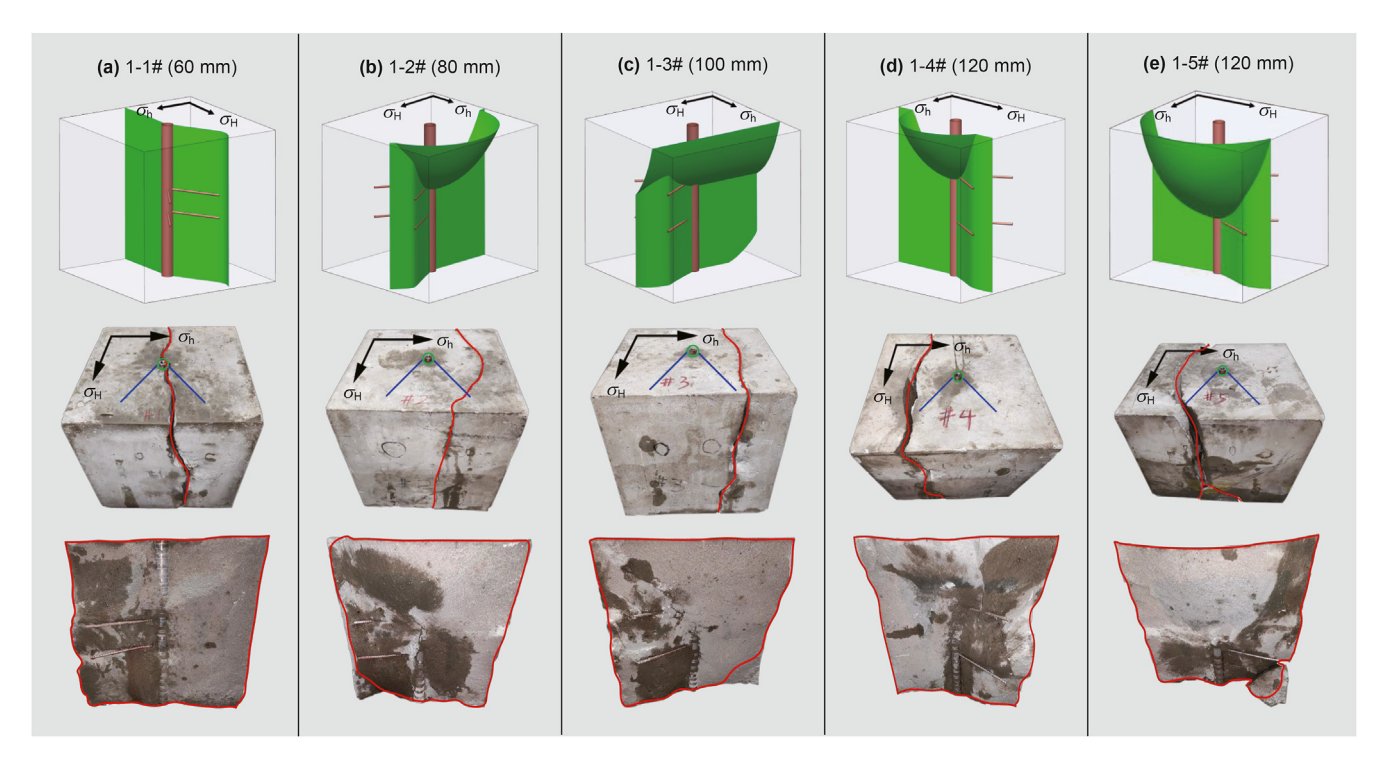


Fig. 9. Fracture geometries with changing vertical distances during radial borehole fracturing in two layers (diameter of 5 mm and azimuth of 30°). Green surfaces represent the fractures, and brown cylinders represent the wellbores. Green circles represent the layouts of the main wellbores, blue lines represent the directions of the radial boreholes, and red curves represent the fracture contours. If other pictures in this paper contain the above icons, the meanings of such icons are identical, and the description of these icons will be omitted

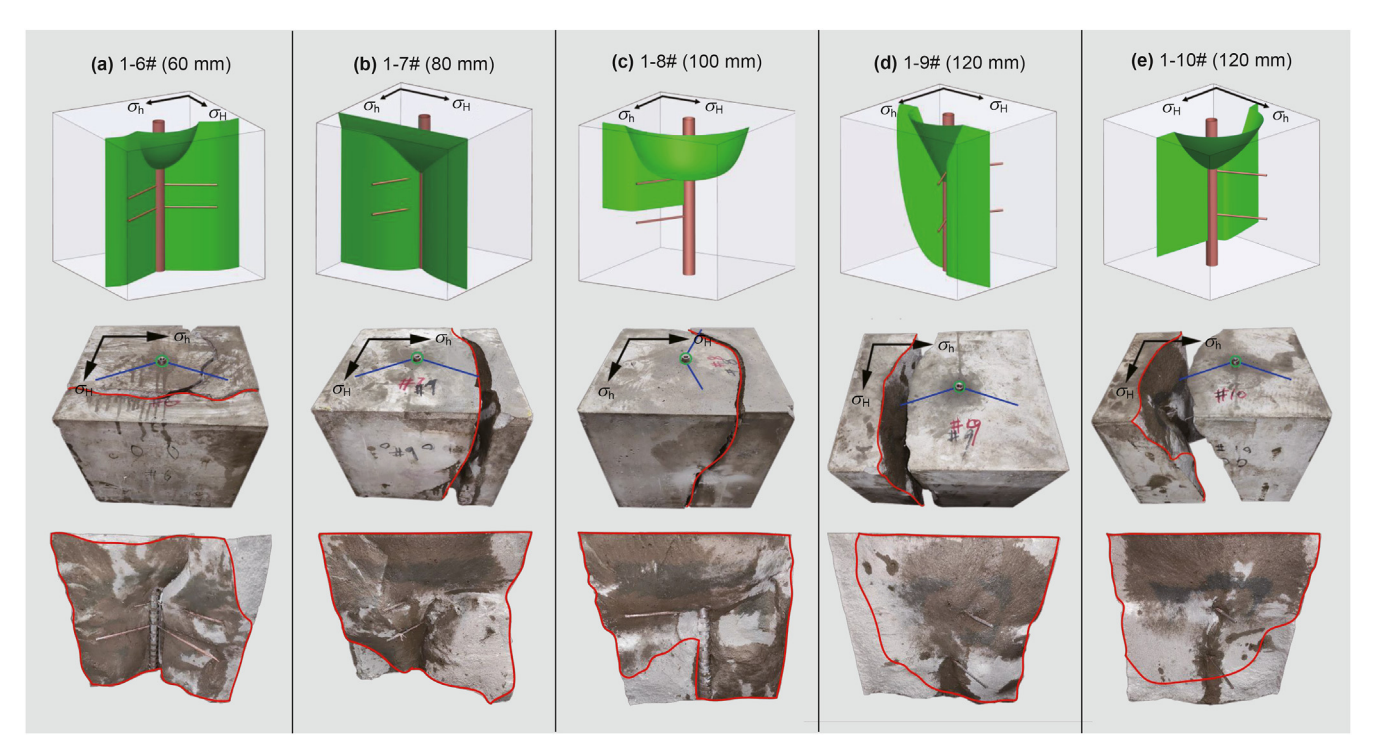


Fig. 10. Fracture geometries with changing vertical distances during radial borehole fracturing in two layers (diameter of 5 mm and azimuth of 60°).

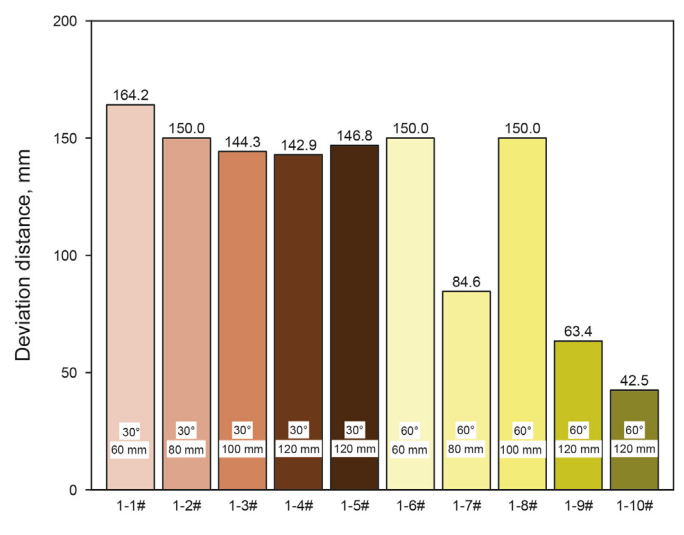


Fig. 11. Deviation distances with changing vertical distances during radial borehole fracturing in two layers (diameter of 5 mm). Numbers in the white boxes are parameter values for the azimuth and vertical distance. If other pictures in this paper contain the above icons, the meanings of such icons are identical, and the description of these icons will be omitted in the captions.

respectively, both at the vertical distance of 120 mm. For samples with the azimuth of 60° , the maximum breakdown pressure is 27.3 MPa at the vertical distance of 60 mm, while the minimum breakdown pressure is 23.6 MPa at the vertical distance of 120 mm. Overall, the breakdown pressures of samples are relatively lower when fracturing radial boreholes with the azimuth of 30° compared to 60° .

3.1.2. Effect of the diameter

To explore the effect of the radial borehole diameter on fracture propagation, we conducted experiments with the diameter of

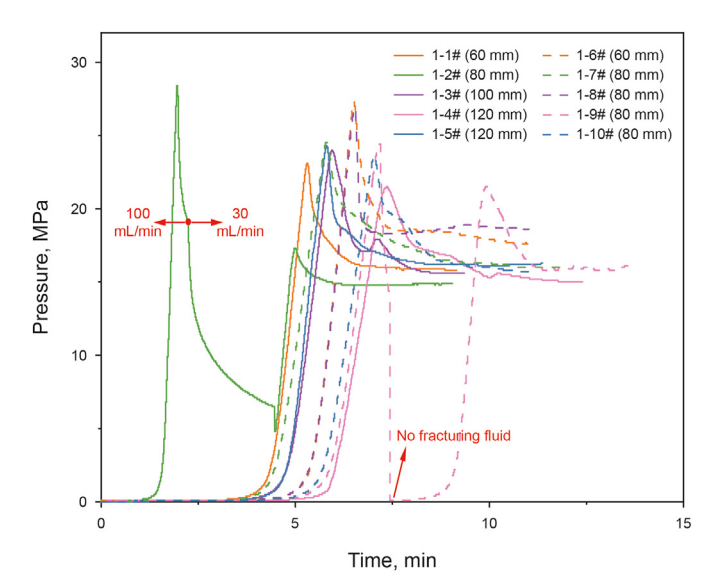


Fig. 12. Fracturing curves with changing vertical distances during radial borehole fracturing in two layers (diameter of 5 mm). The legend includes the test number and vertical distance. If other pictures in this paper contain the above icons, the meanings of such icons are identical, and the description of these icons will be omitted in the captions.

10 mm at vertical distances of 80, 100, and 120 mm, while also accounting for the effect of the azimuth.

Fracture geometries. When the azimuth is 30° , regardless of the vertical distance within the range of 80-120 mm, fractures connecting two radial borehole layers are generated in all samples, as shown in Fig. 14. This phenomenon is also observed in the samples 1-1# to 1-4#, which also with the azimuth of 30° . When the azimuth is 60° , fracture geometries are various as the vertical distance changes. When the vertical distance is 80 mm, the fracture

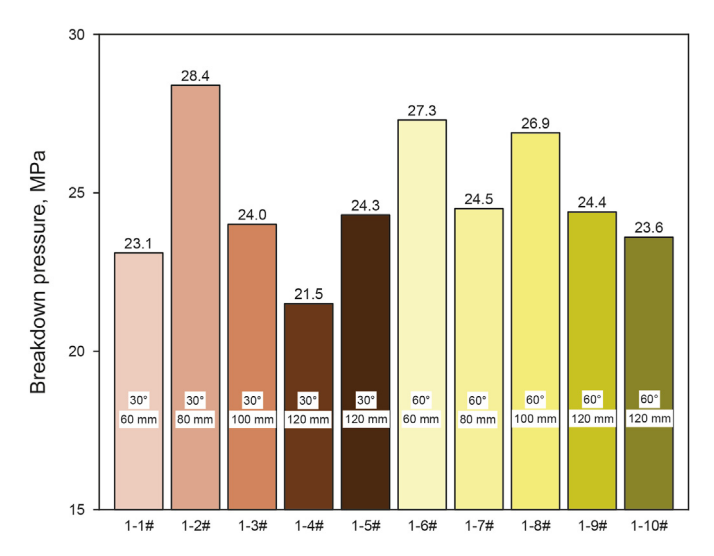


Fig. 13. Breakdown pressures with changing vertical distances during radial borehole fracturing in two layers (diameter of 5 mm).

connects two radial borehole layers in a row (Fig. 15(a)). As the vertical distance rises to 100 mm, the fracture passes through two radial borehole layers on the left side and then curves to the minimum horizontal stress direction. Another fracture cuts through the bottom radial borehole on the right side and gradually propagates towards the maximum horizontal stress direction (Fig. 15(b)). As the vertical distance rise to 120 mm, the fractures cannot pass through the radial boreholes (Fig. 15(c) and (d)).

Deviation distances. Fig. 16 shows the deviation distances of samples 1-11# to 1-18#. When the azimuth is 30° , the deviation distances are consistently 150 mm. With the azimuth of 60° , the deviation distances show a significant decrease compared to the azimuth of 30° . In particular, the deviation distances are zero as the

vertical distance rises to 120 mm. Comparing Figs. 11 and 16, it is concluded that for the azimuth of 30° , the deviation distance increases with an increase in diameter; while for the azimuth of 60° , the deviation distance decreases with an increase in diameter.

Breakdown pressures. The fracturing curves and breakdown pressures of samples 1-11# to 1-18# are shown in Figs. 17 and 18. When the azimuth is 30°, the maximum and minimum breakdown pressures are 25.6 and 19.4 MPa, respectively, both at the vertical distance of 120 mm. Increasing the vertical distance from 80 to 120 mm results in a decrease in the breakdown pressures from 23.6 to 19.4 MPa. When the azimuth is 60°, the maximum breakdown pressure is 25.0 MPa at the vertical distance of 80 mm, while the minimum breakdown pressure is 21.1 MPa at the vertical distance of 120 mm. Increasing the vertical distance from 80 to 120 mm also results in a decrease in the breakdown pressures from 25 to 21.1 MPa. If the fracture initiation position changes from the heel to the toe of radial boreholes, the breakdown pressures will decrease (Liu et al., 2018a). But the breakdown pressure of sample 1-17# exceeds expectations. The reason will be analyzed in the following section

3.2. Radial borehole fracturing in three layers

This set of experiments investigates fracture geometries and breakdown pressures when fracturing radial boreholes in three layers. We conducted experiments with three different vertical distances (60, 80, and 100 mm) and two different azimuths (30° and 60°).

Fracture geometries. When the azimuth is 30° , as the vertical distance varies from 60 to 100 mm, fractures connect three layers of radial boreholes in a row (Fig. 19(a)-(c)), similarly to fractures observed when fracturing radial boreholes in two layers (the azimuth of 30°). When the vertical distance is 100 mm, the fracture only passes through the single radial borehole in the bottom layer (Fig. 19(d)).

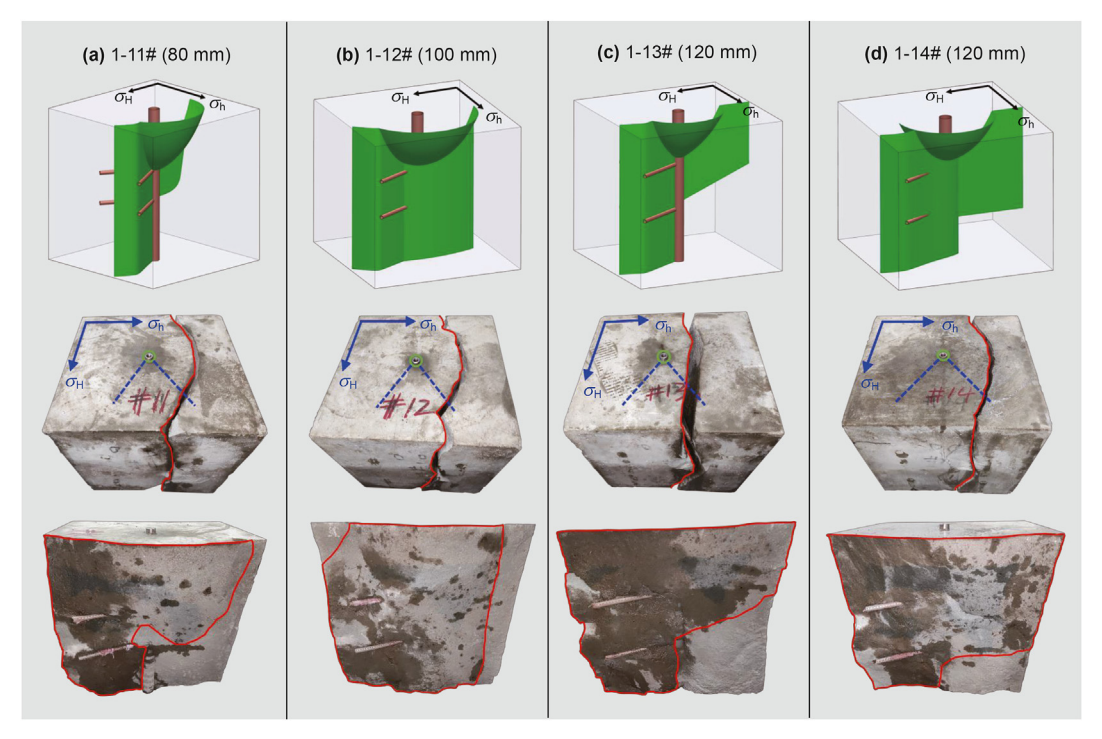


Fig. 14. Fracture geometries with changing vertical distances during radial borehole fracturing in two layers (diameter of 10 mm and azimuth of 30°).

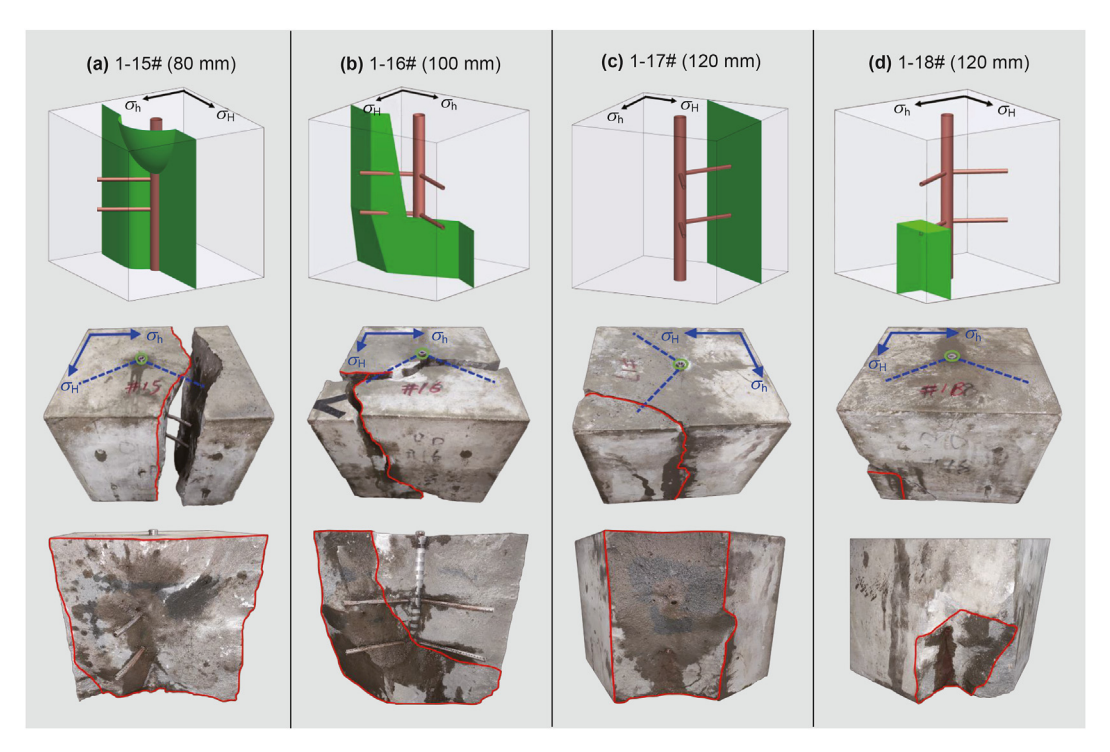


Fig. 15. Fracture geometries with changing vertical distances during radial borehole fracturing in two layers (diameter of 10 mm and azimuth of 60°).

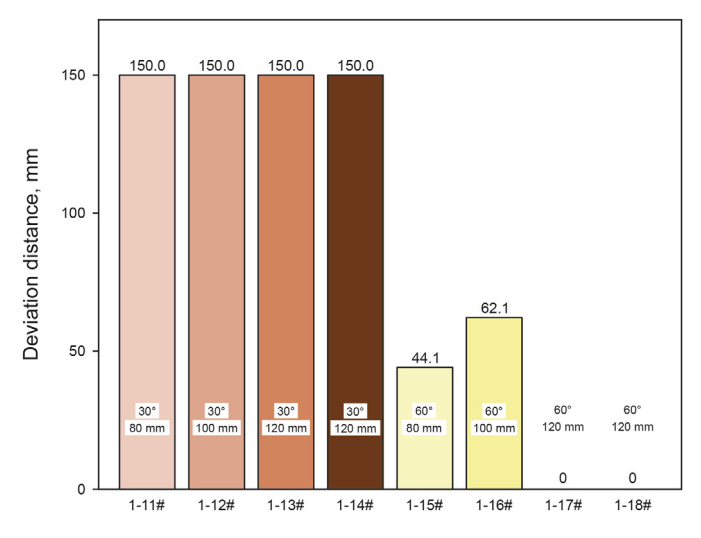


Fig. 16. Deviation distances with changing vertical distances during radial borehole fracturing in two layers (diameter of 10 mm).

When the azimuth is 60° , fracture geometries are various as the vertical distance varies. With the vertical distance of 60 mm, the fracture connects three layers of radial boreholes in a row (Fig. 20(a)). At the vertical distance of 80 mm, the fracture passes through two lower layers of radial boreholes in two rows. Eventually, the fracture curves to the minimum horizontal stress direction, as shown in Fig. 20(b). When the vertical distance rises to 100 mm, the fractures pass through the toe of the radial boreholes instead of passing through their axes (Fig. 20(c) and (d)).

Deviation distances. Fig. 21 indicates the deviation distances of samples 2-1# to 2-8#. The deviation distance of sample 2-6# (150.2 mm) is the highest in this set of experiments. The deviation distance of fractures that pass through a single radial borehole is larger than that of fractures connecting three layers of radial

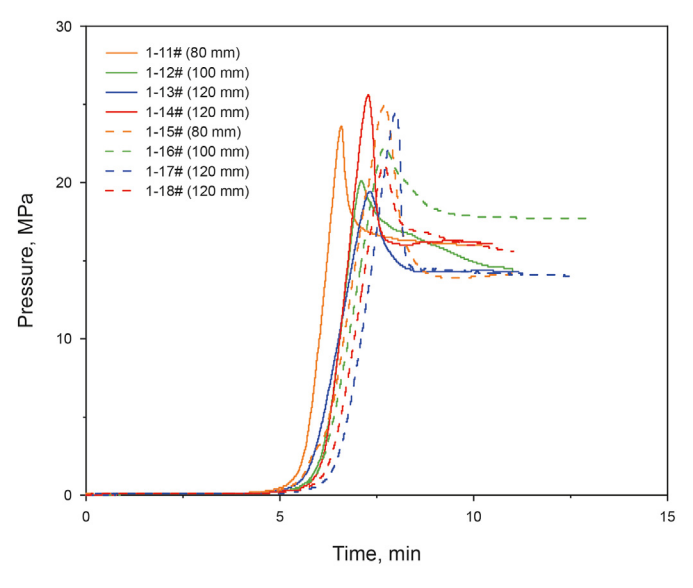


Fig. 17. Fracturing curves with changing vertical distances during radial borehole fracturing in two layers (diameter of 10 mm).

boreholes. For example, the deviation distance of sample 2-4# is 130.0 mm, while that of sample 2-3# is 114.7 mm. In contrast to the azimuth of 60° , deviation distances are generally higher when the azimuth is 30° .

Breakdown pressures. Figs. 22 and 23 show the fracturing curves and breakdown pressures of samples 2-1# to 2-8#. When the azimuth is 30°, increasing the vertical distance from 60 to 100 mm decreases the breakdown pressure from 19.0 to 17.6 MPa. Breakdown pressures decrease when fractures pass through the toes of radial boreholes, such as 13.0 MPa of sample 2-7# and 18.5 MPa of sample 2-8#. Conversely, the breakdown pressure increases when two rows of radial boreholes are fractured, such as

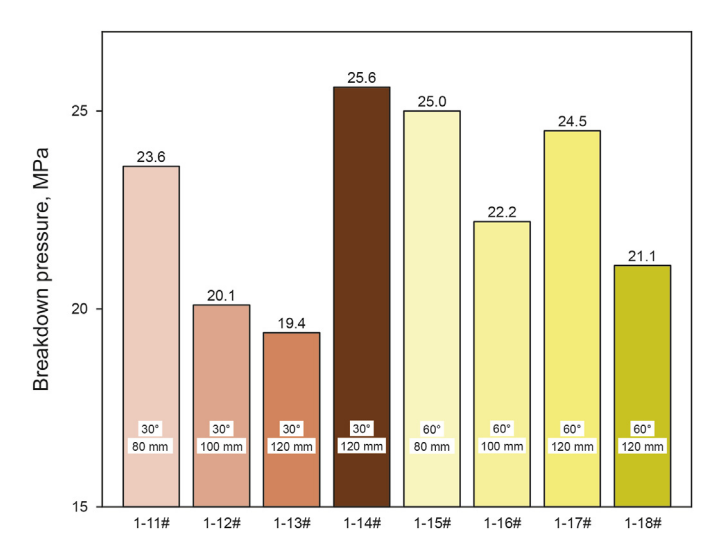


Fig. 18. Breakdown pressures with changing vertical distances during radial borehole fracturing in two layers (diameter of 10 mm).

22.6 MPa of sample 2-6#. Besides, when fractures pass through the radial boreholes, the breakdown pressures of samples with the azimuth of 30° are lower than those with the azimuth of 60°.

4. Discussion

The results of the samples with three radial borehole layers resemble the samples with two radial borehole layers. In this section, we will discuss the results from the entire experiments, including fracture geometry, deviation distance, and breakdown pressure.

4.1. Fracture geometry

Fracture geometries observed in this research are classified into four types according to the connection between hydraulic fractures and radial boreholes, as shown in Fig. 24. Type I fractures connect multiple layers of radial boreholes in two rows. Type II fractures connect multiple layers of radial boreholes in one row. Type III fractures pass through a single radial borehole. Type IV fractures pass through the toes of radial boreholes. The number of samples with four fracture types is summarized in terms of the vertical distance, azimuth, and diameter, as shown in Table 2. The occurrences of Types I—IV fractures among the total fractures account for 11.5% (3/26), 61.5% (16/26), 11.5% (3/26), and 15.5% (4/26), respectively.

The vertical distance is a crucial factor that prominently affects fracture propagation perpendicular to the radial borehole axes. When the vertical distances are 60 and 80 mm, all fractures connect multiple radial borehole layers. However, as the vertical distance increases, fractures tend to preferentially propagate along a single radial borehole or pass through the toes of radial boreholes. For instance, when the vertical distances are 100 and 120 mm, the proportions of fractures connecting multi-layer radial boreholes are 50% (4/8) and 62.5% (5/8), respectively. Increasing the vertical distance weakens the ability of fractures to connect multi-layer radial boreholes. Influenced by the free surface of the top steel plate of the experimental device, crooked fractures are generated at the top of the samples. It is noted that this influence is slight when the vertical distance is relatively small, as demonstrated in sample 1-1# (the vertical distance of 60 mm).

The azimuth significantly affects fracture propagation parallel to the axes of radial boreholes. Increasing the azimuth declines the ability of radial boreholes to guide fractures propagating along their axes. When the azimuth is 30°, fractures of all samples propagate along the radial borehole axes. But when the azimuth is 60°, fractures of four samples cannot pass through radial boreholes. Moreover, with the azimuth of 60° and a relatively large vertical

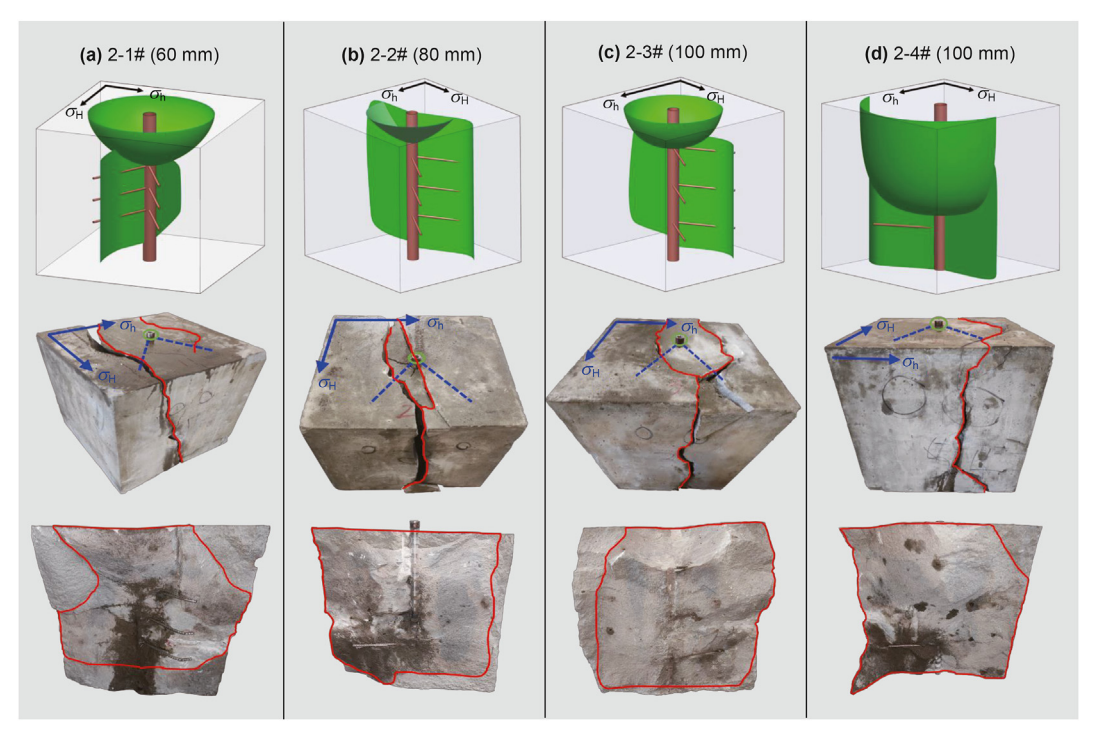


Fig. 19. Fracture geometries with changing vertical distances during radial borehole fracturing in three layers (azimuth of 30°).

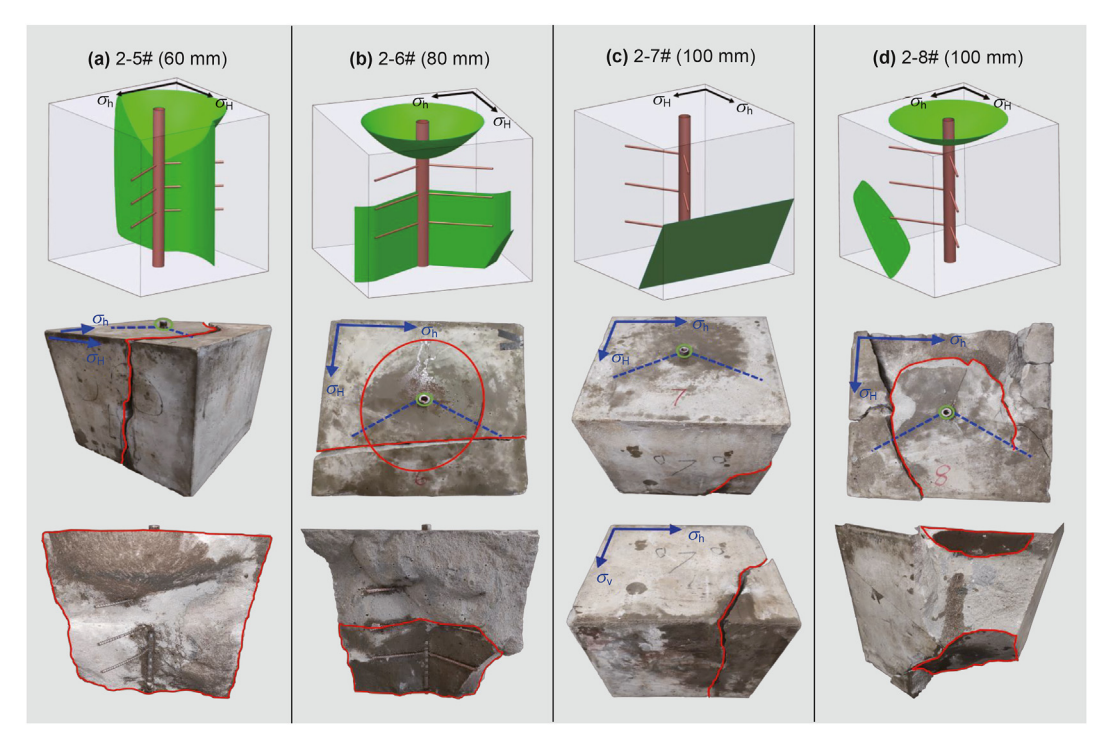


Fig. 20. Fracture geometries with changing vertical distances during radial borehole fracturing in three layers (azimuth of 60°).

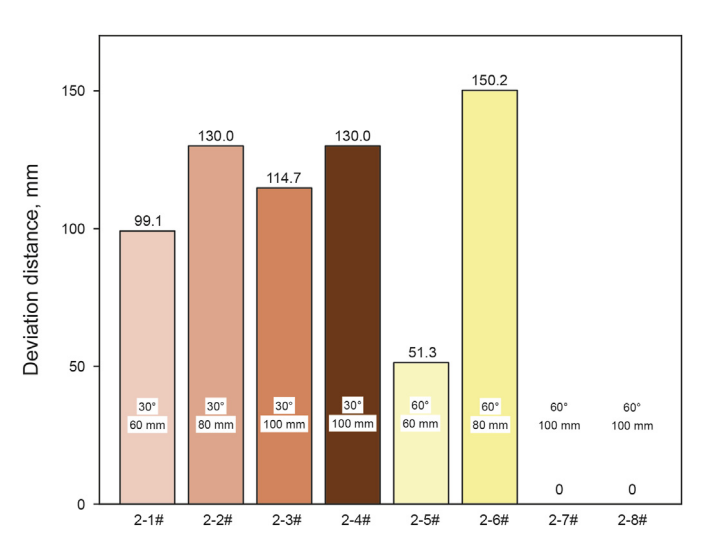


Fig. 21. Deviation distances with changing vertical distances during radial borehole fracturing in three layers.

distance, the fractures will rapidly curve to the maximum horizontal stress direction, as shown in samples 1-9# and 1-10# (the azimuth of 60° and the vertical distance of 120 mm).

Fractures commonly propagate parallel to the maximum horizontal stress direction (Hubbert and Willis, 1957). In this research, when two rows of radial boreholes are fractured, fractures initially propagate along the radial borehole axes and then curve towards the minimum horizontal stress direction, as illustrated in sample 1-6# (the vertical distance of 60 mm, the diameter of 5 mm, and the azimuth of 60°), sample 1-16# (the vertical distance of 100 mm, the diameter of 10 mm, and the azimuth of 60°), and sample 2-6# (the vertical distance of 80 mm, the diameter of 5 mm, and the azimuth of 60°). This phenomenon is consistent with previous research on radial borehole fracturing, which has shown the presence of the

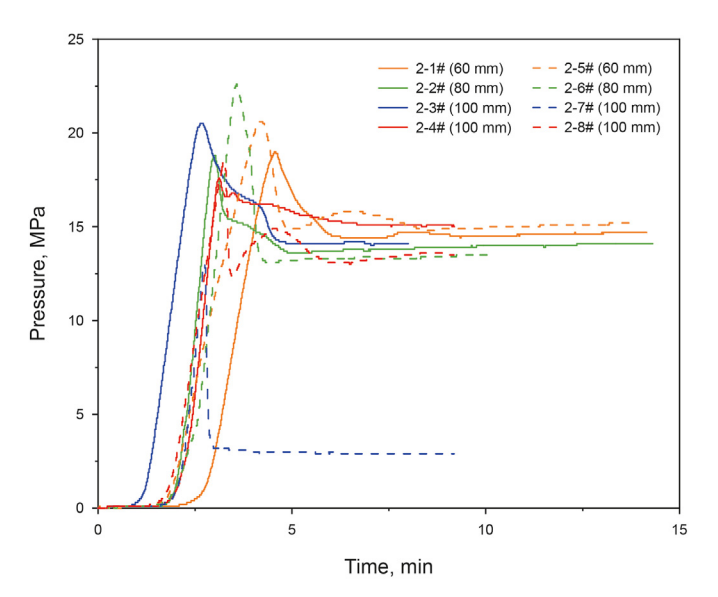


Fig. 22. Fracturing curves with changing vertical distances during radial borehole fracturing in three layers.

extrusion force between the adjacent fractures formed in two rows of radial boreholes (Guo et al. 2019, 2022). When two adjacent fractures propagate simultaneously, the redistribution of stress between fractures causes extrusion force, resulting in the fractures propagating away from each other (Sesetty and Ghassemi, 2015). A similar phenomenon occurs in multi-stage fracturing of horizontal wells, where two adjacent fractures exhibit the same behavior, as shown in Fig. 25 (Wong et al., 2013; Wu and Olson, 2015). In our experimental condition, the extrusion force is favorable for fracture propagation along the radial borehole axes. Additionally, the reason that the fractures do not eventually curve to the maximum horizontal stress direction is the limitation the sample size.

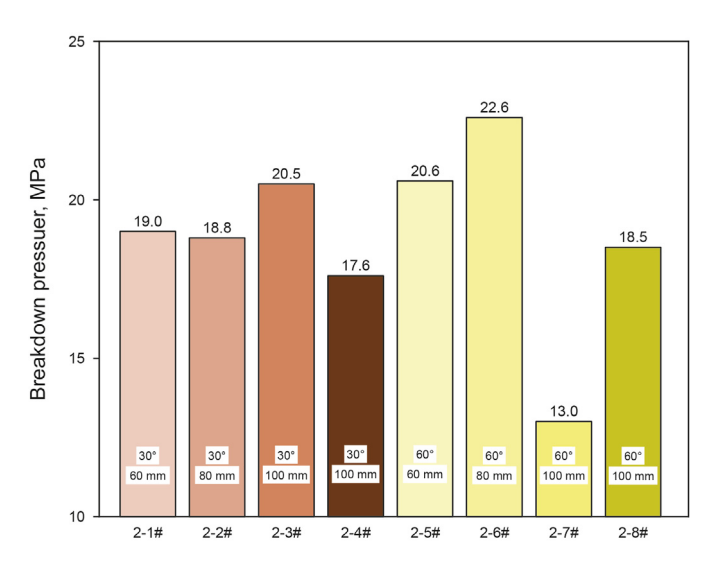


Fig. 23. Breakdown pressures with changing vertical distances during radial borehole fracturing in three layers.

4.2. Deviation distance

The deviation distances are related to fracture geometries. For Type I fractures that connect multiple layers of radial boreholes in two rows, the extrusion force lessens the influence of *in-situ* stress. This strengthens the guiding ability of radial boreholes, leading to an increase in deviation distance. Three samples (1-6#, 1-16#, and 2-6#) with Type I fractures have the largest deviation distances in the set of experiments with only vertical distances varying, as shown in Fig. 26. For Type II fractures that connect multiple layers of radial boreholes in one row, increasing the vertical distance

declines the deviation distances, which decreases 71.7% (from 150 to 42.5 mm) as the vertical distance increases from 60 to 120 mm (Fig. 11). For Type III fractures that pass through a single radial borehole, the deviation distance lifts even though the vertical distance increases. For instance, the deviation distance of sample 1-8# (the vertical distance of 100 mm) is 150.0 mm, while the deviation distance of sample 1-7# (the vertical distance of 80 mm) is 84.6 mm. In this situation, the fracturing fluid is more concentrated. which increases the pressure in the radial borehole and greatly changes the stress condition nearby. Therefore, the maximum stress of the rock near the radial boreholes is more likely to exceed the tensile strength of rock, prompting fractures to preferentially propagate along the axes of the radial boreholes. For Type IV fractures that pass through the toes of radial boreholes, the deviation distances are zero. The reason is that the samples with type IV fractures have the maximum vertical distances in the set of experiments with vertical distances varying. The radial boreholes are situated closer to the rock boundaries. Fractures are easily influenced by the rock boundaries and cannot extend along the radial borehole axes.

The azimuth significantly affects the deviation distances. Compared with samples with the azimuth of 60° , the deviation distances are generally higher than those with the azimuth of 30° . Fig. 27 indicates the deviation distances of the samples featuring Type II fractures. The only differing factor between the two compared samples is the azimuth. It shows that as the azimuth rises from 30° to 60° , the dropping percentage of deviation distances ranges from 43.6% to 70.6% (54.5% on average). Meanwhile, when the azimuth is 60° , the deviation distances become zero when the vertical distances are 100 mm (samples 2-7# and 2-8#) and 120 mm (samples 1-17# and 1-18#), which means that the radial borehole loses its ability to guide fractures propagating along its axes.

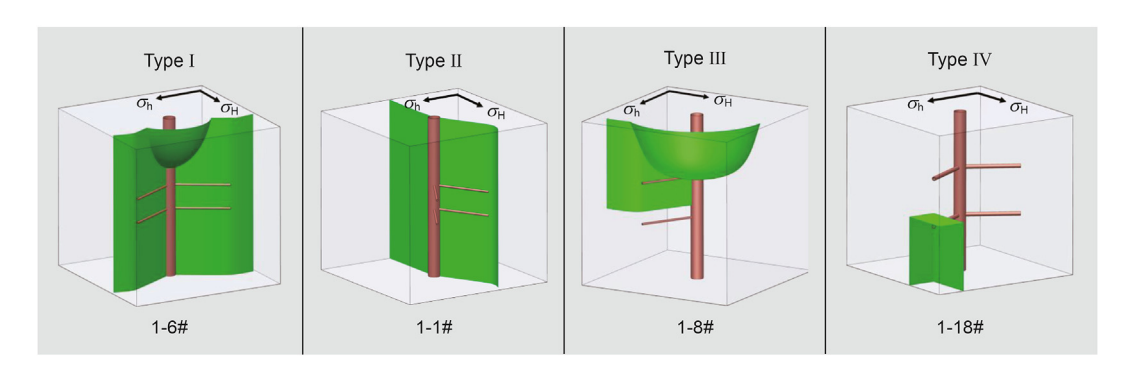


Fig. 24. The typical samples with four types of fractures.

Table 2The number of samples with various fracture geometries.

| Parameter | | The number of samples with the four fracture types | | | | |
|-----------------------|------------------|--|---------|----------|---------|--|
| | | Type I | Type II | Type III | Type IV | |
| Vertical distance, mm | 60 | 1 | 3 | 0 | 0 | |
| | 80 | 1 | 5 | 0 | 0 | |
| | 100 | 1 | 3 | 2 | 2 | |
| | 120 | 0 | 5 | 1 | 2 | |
| Azimuth, degree | 30 | 0 | 11 | 2 | 0 | |
| | 60 | 3 | 5 | 1 | 4 | |
| Diameter, mm | 5 (two layers) | 1 | 7 | 2 | 0 | |
| | 5 (three layers) | 1 | 5 | 0 | 2 | |
| | 10 (two layers) | 1 | 4 | 1 | 2 | |
| Total | | 3 | 16 | 3 | 4 | |

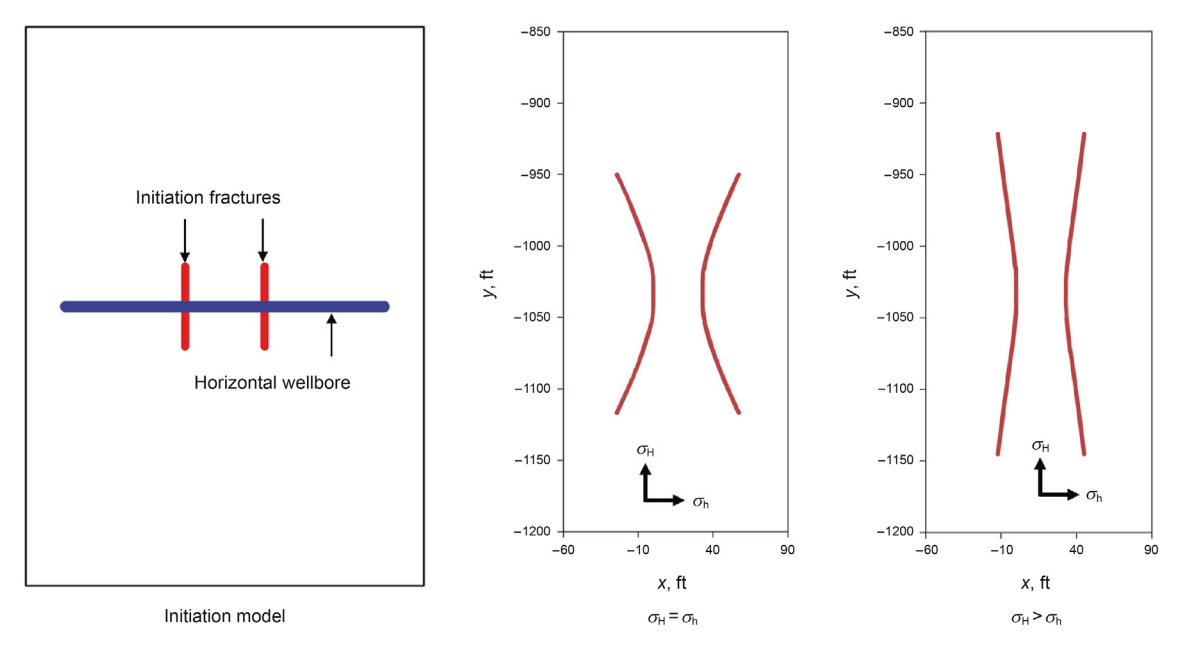


Fig. 25. Dual fracture propagation in horizontal well simultaneous fracturing (Wu and Olson, 2015).

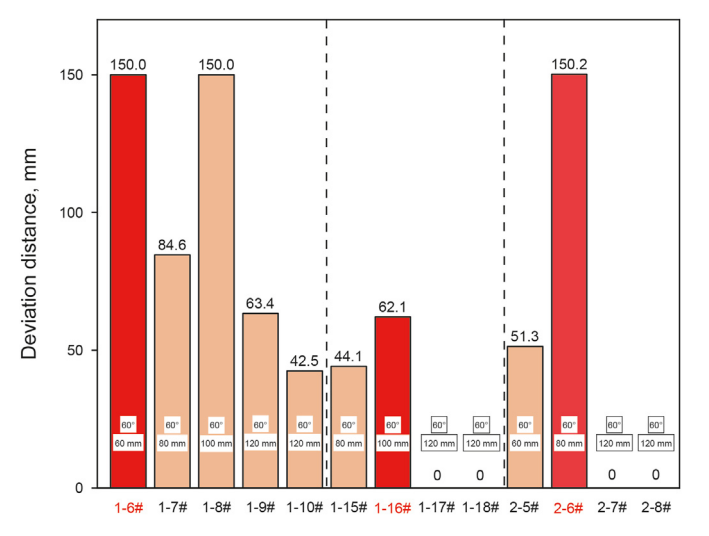


Fig. 26. Deviation distances of three sets of experiments with changing vertical distances.

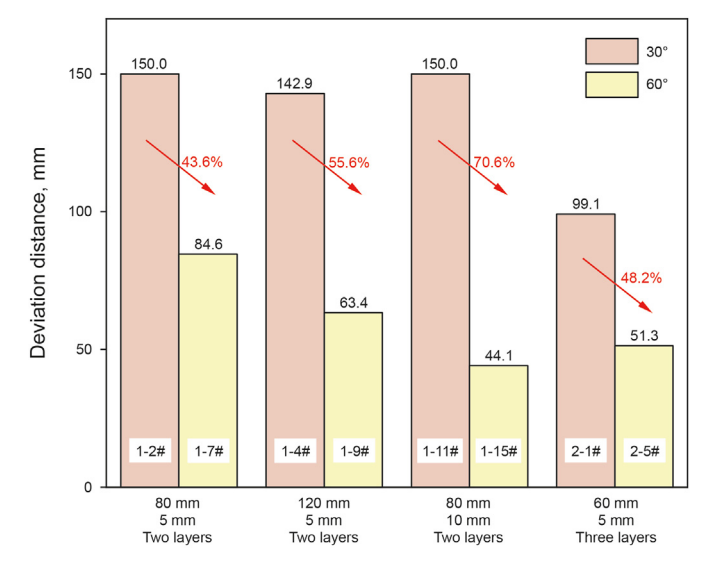


Fig. 27. Deviation distances with the same layers, vertical distance and diameter, and different azimuths.

4.3. Breakdown pressure

The breakdown pressure is correlated with diverse fracture geometries. When fractures connect multi-layer radial boreholes, increasing the vertical distance decreases the breakdown pressure. The breakdown pressure decreases by 17.8% (from 23.6 to 19.4 MPa) as the vertical distance increases from 80 to 120 mm (Fig. 18). The breakdown pressures of certain samples lift due to the complexity of fractures, such as the separate crooked fracture in sample 2-6#, and the fracture that only passes through the axis of the first half of the radial borehole in sample 1-14#. Because fracture propagation exhibits unstable propagation in the laboratory experiment. Fractures form suddenly after the accumulation of a significant number of microcracks (Fineberg et al., 1992). The more complexity of the fracture requires the accumulation of more energy, resulting in higher breakdown pressure. Among the samples with changing vertical distances, those exhibiting Type III fractures tend to have

relatively higher breakdown pressures. Because the fracture initiation and propagation also need more hydraulic energy in one radial borehole compared to multiple radial boreholes. The breakdown pressures of samples with Type IV fractures are relatively small (samples 1-18#, 2-7#, and 2-8#), which is consistent with previous research (Liu et al., 2018a). Besides, if the fracture passes through the toes of two radial boreholes (sample 1-19#) or the more complex fracture is generated (sample 2-8#), the breakdown pressures are enhanced.

Increasing the azimuth rises the breakdown pressure. Given the correlations between breakdown pressures and fracture geometries, we conducted an analysis on samples with different azimuths, all of which display Type II fractures. As shown in Fig. 28, as the azimuth increases from 30° to 60° , the rising percentage of breakdown pressure ranges from 5.9% to 13.5% (9.3% on average). With an increase in azimuth, the interference stress produced by

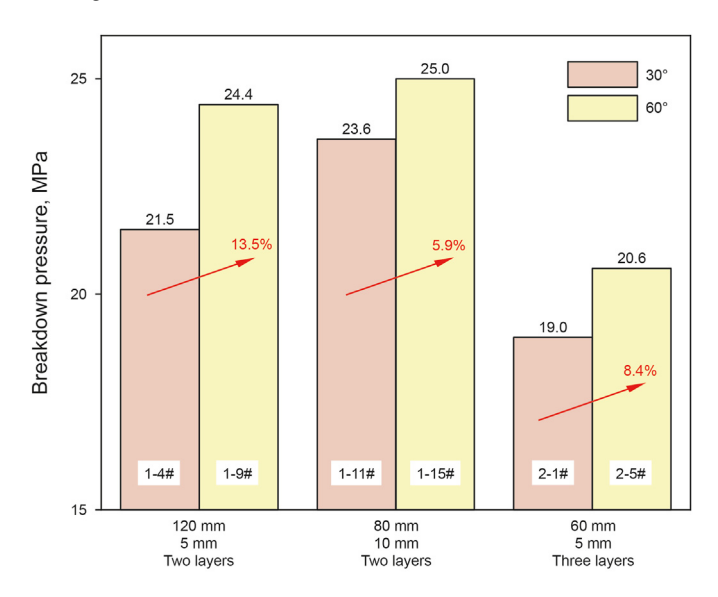


Fig. 28. Breakdown pressures with the same layers, vertical distance and diameter, and different azimuths.

adjacent radial boreholes decreases. So, the propagation of fractures requires the accumulation of more hydraulic energy.

Fig. 29 compares the breakdown pressures of the samples with varying diameters. The breakdown pressure of the sample with maximum vertical distance in each group is the average of the two repeated experiments. It is obvious that increasing the diameter decreases the breakdown pressure. In the context of longitudinally propagating of fractures during radial borehole fracturing, fractures always initiate from symmetrical positions both above and below the heel of the radial boreholes, where they bear tensile stress (Liu et al. 2017, 2018a). For multiple radial borehole layers, the stress zones between these layers is the superimposition of the respective effects (Tian et al., 2017). Increasing the diameter enhances the superimposition of the zones that bear tensile stress near radial boreholes. So, the maximum stress of the rock around radial boreholes easily exceeds its tensile strength, and fractures can

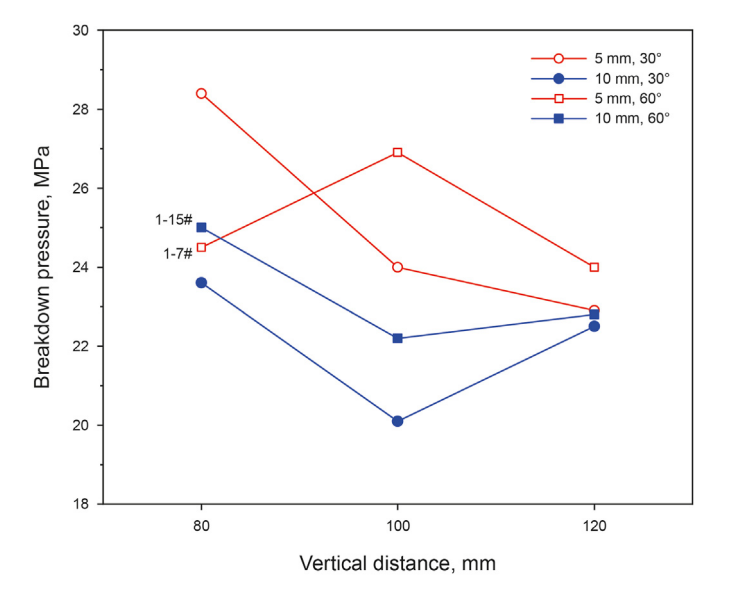


Fig. 29. Breakdown pressures when changing vertical distances with various diameter and azimuth.

initiate at a lower breakdown pressure. Possibly there is a defect in sample 1-7#, the breakdown pressure of sample 1-7# (24.5 MPa, the diameter of 5 mm) is lower than that of sample 1-15# (25.0 MPa, the diameter of 10 mm).

5. Conclusions

In this work, we conducted a series of experiments of radial borehole fracturing in multiple layers to investigate the unique fracture propagation and pressure characteristics. Three crucial factors corresponding to the vertical distance of adjacent radial borehole layers, the azimuth and diameter of radial borehole are investigated. The deviation distance and breakdown pressure are employed as quantitative measures to assess the fracture propagation and pressure characteristics. The main conclusions are summarized as follows.

- (1) Radial borehole fracturing in multiple layers generates diverse fracture geometries. Based on the connectivity between hydraulic fractures and radial boreholes, four types of fractures are observed, corresponding to Type I fracture that connects multi-layer radial boreholes in multiple rows, Type II fracture that connects multi-layer radial boreholes in a single row, Type III fracture that passes through the single radial borehole, and Type IV fracture that passes through the toes of radial boreholes.
- (2) The vertical distance significantly influences fracture propagation perpendicular to the radial borehole axes, while the azimuth affects fracture propagation parallel to them. Increasing the vertical distance hinders the fracture from connecting multiple radial borehole layers. Specifically, the fracture may not be able to connect multiple layers of radial boreholes when the vertical distance is relatively large. Increasing the azimuth declines the guiding ability of radial boreholes, which makes the fracture quickly curve to the maximum horizontal stress direction.
- (3) If the fracture can connect multi-layer radial boreholes, the increase in the vertical distance will decrease the deviation distance, which decreases by 71.7% as the vertical distance increases from 60 to 120 mm. Increasing the azimuth can also have a negative impact on the deviation distance, with an average drop of 54.5% as the azimuth rises from 30° to 60°.
- (4) The breakdown pressures correlate with diverse fracture geometries and are influenced by the complexity of fractures. When the fracture connects multi-layer radial boreholes, increasing the vertical distance decreases the breakdown pressure. When the fracture initiates and propagates in a single radial borehole, the breakdown pressure lifts. When the fracture initiates and propagates on the toes of radial boreholes, the breakdown pressure decreases. The azimuth has a positive effect on the breakdown pressure. As the azimuth rises from 30° to 60°, the breakdown pressure rises 9.3% on average. Additionally, increasing the diameter decreases the breakdown pressure.
- (5) The extrusion force exists between the adjacent fractures generated in radial boreholes in multiple rows, which contributes to enhancing the guiding ability of radial boreholes and results in higher breakdown pressure.

Declaration of competing interest

No conflict of interest exists in the submission of this manuscript, and the manuscript is approved by all authors for publication.

Acknowledgment

The authors gratefully acknowledge the financial support received from the Strategic Cooperation Technology Projects of CNPC and CUPB (No. ZLZX2020-01) and the National Key Scientific Research Instrument Research Project of NSFC (No. 51827804).

References

- Abass, H.H., Soliman, M.Y., Al-Tahini, A.M., et al., 2009. Oriented fracturing: a new technique to hydraulically fracture an openhole horizontal well. In: SPE Annual Technical Conference and Exhibition. https://doi.org/10.2118/124483-MS.
- Bai, Y., Liu, S.Q., Xia, Z.H., et al., 2021. Fracture initiation mechanisms of multi-branched radial-drilling fracturing. Lithosphere. https://doi.org/10.2113/2021/3316083.
- Bruni, M.A., Biasotti, J.H., Salomone, G.D., 2007. Radial drilling in Argentina. In: Latin American & Caribbean Petroleum Engineering Conference. https://doi.org/ 10.2118/107382-MS.
- Cinelli, S.D., Kamel, A.H., 2013. Novel technique to drill horizontal laterals revitalizes aging field. In: SPE/IADC Drilling Conference. https://doi.org/10.2118/163405-
- Cirigliano, R.A., Talavera Blacutt, J.F., 2007. First experience in the application of radial perforation technology in deep wells. In: Latin American & Caribbean Petroleum Engineering Conference. https://doi.org/10.2118/107182-MS.
- Fineberg, J., Gross, S.P., Marder, M., et al., 1992. Instability in the propagation of fast cracks. Phys. Rev. B 45 (10), 5146. https://doi.org/10.1103/PhysRevB.45.5146.
- Fu, X., Li, G.S., Huang, Z.W., et al., 2015. Experimental and numerical study of radial lateral fracturing for coalbed methane. J. Geophys. Eng. 12 (5), 875–886. https:// doi.org/10.1088/1742-2132/12/5/875.
- Gong, D.G., Qu, Z.Q., Guo, T.K., et al., 2016. Variation rules of fracture initiation pressure and fracture starting point of hydraulic fracture in radial well. J. Petrol. Sci. Eng. 140, 41–56. https://doi.org/10.1016/j.petrol.2016.01.006.
- Guo, T.K., Gong, F.C., Shen, L., et al., 2019. Multi-fractured stimulation technique of hydraulic fracturing assisted by radial slim holes. J. Petrol. Sci. Eng. 174, 572–583. https://doi.org/10.1016/j.petrol.2018.11.064.
- Guo, T.K., Liu, B.Y., Qu, Z.Q., et al., 2017a. Study on initiation mechanisms of hydraulic fracture guided by vertical multi-radial boreholes. Rock Mech. Rock Eng. 50 (7), 1767–1785. https://doi.org/10.1007/s00603-017-1205-3.
- Guo, T.K., Qu, Z.Q., Gong, D.G., et al., 2016. Numerical simulation of directional propagation of hydraulic fracture guided by vertical multi-radial boreholes. I. Nat. Gas Sci. Eng. 35, 175–188. https://doi.org/10.1016/j.ingse.2016.08.056.
- J. Nat. Gas Sci. Eng. 35, 175–188. https://doi.org/10.1016/j.jngse.2016.08.056.
 Guo, T.K., Qu, Z.Q., Gong, F.C., et al., 2017b. Numerical simulation of hydraulic fracture propagation guided by single radial boreholes. Energies 10 (10), 1680. https://doi.org/10.3390/en10101680.
- Guo, Z.Q., Tian, S.C., Liu, Q.L., et al., 2022. Experimental investigation on the breakdown pressure and fracture propagation of radial borehole fracturing.

 Lettel Sci. Eng. 208. 109169. https://doi.org/10.1016/j.petrol.2021.109169.
- J. Petrol. Sci. Eng. 208, 109169. https://doi.org/10.1016/j.petrol.2021.109169. Huang, Z., Huang, Z.W., Su, Y.A., et al., 2020a. A feasible method for the trajectory measurement of radial jet drilling laterals. SPE Drill. Complet. 35 (1), 125–135. https://doi.org/10.2118/192140-PA.
- Huang, Z., Huang, Z.W., Wu, L., et al., 2020b. Trajectory measurement of radial jet drilling wells: improved tool and data processing. J. Energy Resour. Technol. 142 (3), 032902. https://doi.org/10.1115/1.4044622.
- Hubbert, M.K., Willis, D.G., 1957. Mechanics of hydraulic fracturing. Transac. AIME 210, 153–168. https://doi.org/10.2118/686-G.
- Kamel, A.H., 2016. RJD: a cost effective frackless solution for production enhancement in marginal fields. In: SPE Eastern Regional Meeting. OnePetro. https://doi.org/10.2118/184053-MS.
- Landers, C.W., 1998. Method of and apparatus for horizontal well drilling. US Patents 5853056.
- Li, Y.H., Wang, C.J., Shi, L.H., et al., 2000. Application and development of drilling and completion of the ultrashort-radius radial well by high pressure jet flow

- techniques. In: International Oil and Gas Conference and Exhibition in China. https://doi.org/10.2118/64756-MS.
- Liu, G.Q., Ehlig-Economides, C., 2016. Interpretation methodology for fracture calibration test before-closure analysis of normal and abnormal leakoff mechanisms. In: SPE Hydraulic Fracturing Technology Conference. https://doi.org/ 10.2118/179176-MS.
- Liu, Q.L., Tian, S.C., 2020. 3D numerical modeling of fracture initiation from branch wellbore. Energy Sources Part A 1–20. https://doi.org/10.1080/15567036.2020.1795316.
- Liu, Q.L., Tian, S.C., Li, G.S., et al., 2017. Hydraulic fracture initiation from radial lateral borehole. In: 51st US Rock Mechanics/Geomechanics Symposium.
- Liu, Q.L., Tian, S.C., Li, G.S., et al., 2018a. An analytical model for fracture initiation from radial lateral borehole. J. Petrol. Sci. Eng. 164, 206–218. https://doi.org/ 10.1016/j.petrol.2018.01.056.
- Liu, Q.L., Tian, S.C., Li, G.S., et al., 2018b. Fracture initiation and propagation characteristics for radial drilling-fracturing: an experimental study. In: Unconventional Resources Technology Conference. https://doi.org/10.15530/urtec-2018-2902984.
- Liu, X.Q., Qu, Z.Q., Guo, T.K., et al., 2019. An innovative technology of directional propagation of hydraulic fracture guided by radial holes in fossil hydrogen energy development. Int. J. Hydrogen Energy 44 (11), 5286–5302. https://doi.org/10.1016/j.ijhydene.2018.07.189.
- Maut, P.P., Jain, D., Mohan, R., et al., 2017. Production enhancement in mature fields of Assam Arakan basin by radial jet drilling-a case study. In: SPE Symposium: Production Enhancement and Cost Optimisation. OnePetro. https://doi.org/10.2118/189243-MS.
- Ragab, A.M., Kamel, A.M., 2013. Radial drilling technique for improving well productivity in Petrobel-Egypt. In: North Africa Technical Conference and Exhibition. https://doi.org/10.2118/164773-MS.
- Raheem, A.A., Soyingbe, A.A., Emenike, A.J., 2013. Effect of curing methods on density and compressive strength of concrete. Int. J. Appl. Sci. Technol. 3 (4).
- Sesetty, V., Ghassemi, A., 2015. A numerical study of sequential and simultaneous hydraulic fracturing in single and multi-lateral horizontal wells. J. Petrol. Sci. Eng. 132, 65–76. https://doi.org/10.1016/j.petrol.2015.04.020.
- Sun, L.D., Fang, C.L., Li, F., et al., 2010. Petroleum exploration and development practices of sedimentary basins in China and research progress of sedimentology. Petrol. Explor. Dev. 37 (4), 385–396. https://doi.org/10.1016/S1876-3804(10)60040-7.
- Sun, L.D., Zou, C.N., Jia, A.L., et al., 2019. Development characteristics and orientation of tight oil and gas in China. Petrol. Explor. Dev. 46 (6), 1073–1087. https://doi.org/10.1016/S1876-3804(19)60264-8.
- Tian, Y., Qu, Z.Q., Guo, T.K., et al., 2017. Theoretical research on radial wells orientating hydraulically created fracture directional extended. Int. J. Hydrogen Energy 42 (29), 18358–18363. https://doi.org/10.1016/j.ijhydene.2017.04.179.
- Wang, T.Y., Liu, Q.L., Zhu, B., et al., 2020. Fracture initiation characteristics from multiple radial wellbores. In: 54th US Rock Mechanics/Geomechanics Symposium.
- Wong, S.-W., Geilikman, M., Xu, G.S., 2013. Interaction of multiple hydraulic fractures in horizontal wells. In: SPE Unconventional Gas Conference and Exhibition. https://doi.org/10.2118/163982-MS.
- Wu, G., 2012. Process study on radial drilling technology to exploit CBM in Qinshui basin. China Coal 38 (1), 9–12 (in Chinese).
- Wu, K., Olson, J.E., 2015. Simultaneous multifracture treatments: fully coupled fluid flow and fracture mechanics for horizontal wells. SPE J. 20 (2), 337–346. https://doi.org/10.2118/167626-PA.
- Xian, B.A., Xia, B.R., Zhang, Y., et al., 2010. Technical analysis on radial horizontal well for development of coalbed methane of low coal rank. Coal Geol. Explor. 38 (4), 25–29 (in Chinese).
- Yan, C.L., Cheng, Y.F., Deng, F.C., et al., 2017. Experimental study on the hydraulic fracturing of radial horizontal wells. In: 4th ISRM Young Scholars Symposium on Rock Mechanics.
- Zou, C.N., Yang, Z., He, D.B., et al., 2018. Theory, technology and prospects of conventional and unconventional natural gas. Petrol. Explor. Dev. 45 (4), 604–618. https://doi.org/10.1016/S1876-3804(18)30066-1.